Irradiation Creep Behavior of Vanadium Alloys during Neutron Irradiation in a Liquid Metal Environment

Kenichi FUKUMOTO, Minoru NARUI[1)], Hideki MATSUI[1)], Takuya NAGASAKA[2)] and Takeo MUROGA[2)]

Graduate School of Nuclear Power and Energy Safety Engineering, University of Fukui, Fukui 910-8507, Japan
[1)]*The Oarai Center, Institute for Materials Research, Tohoku Univ., Oarai 310-1313, Japan*
[2)]*National Institute for Fusion Science, Toki 509-5292, Japan*

(Received 30 November 2007 / Accepted 25 February 2008)

The manufacturing process of creep specimens and an irradiation technique in a liquid metal environment for in-pile and creep measurements of irradiated samples are established for highly purified V-4Cr-4Ti, NIFS-HEAT alloys. Irradiation experiments with sodium-enclosed irradiation capsules in JOYO and lithium-enclosed irradiation capsules in HFIR-17J were conducted using pressurized creep tubes.

From thermal creep experiments, the activation energy of creep deformation using pressurized creep tubes was determined to be 210 kJ/mol·K, the creep stress factor was 4.9 for an 800°C creep test, and its mechanism was determined to be a climb-assisted glide of dislocation motion.

It was found that the creep strain rate exhibited a linear relationship with effective stress up to 150 MPa from 425 to 600°C under JOYO and HFIR irradiation. The activation energy of irradiation creep was estimated to be 46 kJ/mol·K. No significant difference in irradiation creep behavior between the liquid sodium and liquid lithium environments was observed. A set of essential physical data of irradiation creep properties was obtained for V-4Cr-4Ti alloys.

Keywords: vanadium alloy, irradiation creep, liquid metal environment, irradiation technique, impurity effect

DOI: 10.1585/pfr.3.017

1. Introduction

Vanadium alloys are attractive candidate materials for fusion reactor blankets because of their potentially high operation temperatures. However, there is limited knowledge about their mechanical properties during neutron irradiation at high temperatures. Irradiation creep deformation is one of the most important issues affecting the lifetime of materials in a fusion reactor [1, 2]. At fusion relevant high temperature, the creep strain rate of the materials can be large when excess point defects are generated by irradiation. Recently, material irradiation technology for use in liquid metal environments has been developed, and irradiation creep experiments in a nuclear pile have been conducted for vanadium alloys. Environmental and irradiation effects of creep deformation in irradiation creep experiments under neutron irradiation should be distinguished independently for understanding the essential irradiation creep process taking place in a pile. Figure 1 shows the process of research and development of irradiation creep behavior of highly purified vanadium alloys under irradiation in liquid metal environments.

In this study, comprehensive reports of the establishment of the manufacturing process of pressurized creep tube and irradiation technique using liquid metal capsules are described. The main objective of this study is to investigate the environmental effects of irradiation creep properties of high-purified V-4Cr-4Ti alloys, i.e., NIFS-HEAT-2 irradiated by neutrons. For conducting irradiation creep tests in a pile, a sodium-enclosed irradiation rig in JOYO

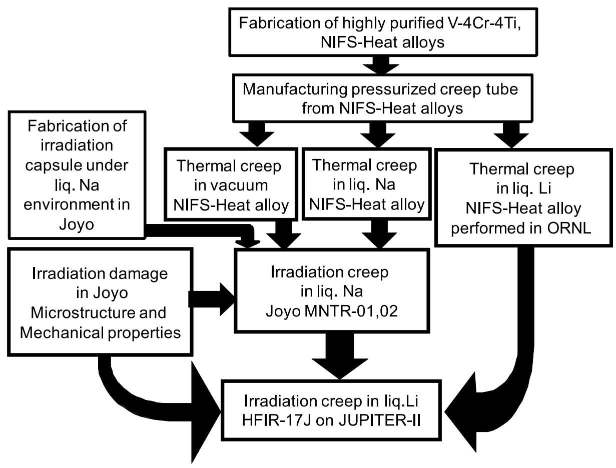

Fig. 1 Research and development in the irradiation creep behavior of highly purified vanadium alloys under irradiation in liquid metal environments.

author's e-mail: fukumoto@mech.fukui-u.ac.jp

and a lithium-enclosed irradiation rig in HFIR-17J were used for pressurized creep tubes (PCTs) of NIFS-HEAT alloys via the suppression of the impurity content during the manufacturing process.

2. Experimental Procedure

2.1 Preparation of pressurized creep tube [3]

The V-4Cr-4Ti alloy used in this study was produced by NIFS and Taiyo Koko Co., and is designated as NIFS-HEAT-2 [4]. Figure 2 shows a flow chart of the manufacturing process for pressurized creep tubes of NIFS-HEAT-2 alloys. The tube processing of NIFS-HEAT-2 alloys was successfully carried out by NIFS and Daido Co. Details of the tubing process have been reported previously [5]. The tubes were cut into pieces of pipes with lengths of 1 inch (25.4 mm). The uptake of oxygen was negligible during the tube fabrication. However, the oxygen content in the creep tubes was less than that in previous creep tubes. A significant reduction in the contamination of interstitial impurities during the tube fabrication process was achieved using the newly developed rolling process and appropriate intermediate annealing. Figure 3 shows a blueprint of a creep tube used in this study. The end plugs were fabricated from a rod using a lathe, and a small hole was bored in the top-end plug via electro-discharge machining. The profile and dimension of the hole in the end plug was restricted due to the requirements of the helium gas enclosure technique. The circumferential plug-to-tube welds were made using an electron beam (EB) welder in vacuum in a machine shop in the Japan Atomic Energy Agency (JAEA), Tokai, Japan. The final heat treatment of the PCTs was performed at 1000°C for 2 h under $< 1 \times 10^{-4}$ Pa vacuum. Helium gas sealing was performed in a helium gas enclosure at the Oarai Center of JAEA, Oarai, Japan. In this helium gas enclosure, a plug pin was not used for the enclosing. The top part of the end plug was melted via a laser shot of 50 kJ, and was solidified around a hole in the top end plug. The gas enclosure was obtained by the solidification of a molten pool around an upper hole in the end plug.

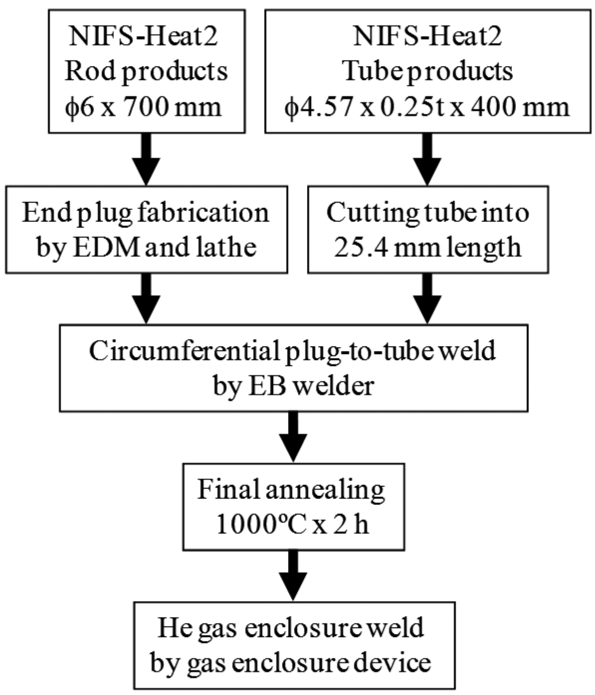

Fig. 2 Manufacturing process of a pressurized creep tube for a NIFS-HEAT-2 alloy.

2.2 Thermal creep experiments under vacuum conditions [6]

The PCTs wrapped with Ta and Zr foils were encapsulated in a quartz tube under a vacuum of $<\sim 5 \times 10^{-3}$ Pa. For removing gas impurities from the quartz tube, approximately 100 cm^2 of Zr foil was used as a getter. Thermal creep tests were conducted by placing the sealed quartz tubes in a muffle furnace. Dimensional changes of the PCTs were measured using a precision laser profilometer manufactured by Keyence, LM-7030MT. Figure 4 shows an example of creep deformation using a pressurized creep tube at 700°C in a vacuum. As creep time increased, the diameter of the tube increased isotropically. The diameters were determined to an accuracy of ±1 μm. When the creep strain exceeded 20%, the test was terminated.

2.3 Capsules for thermal and irradiation creep experiments in a sodium environment [7]

To perform the irradiation test in a sodium environment, sodium bonding capsules were prepared: six capsules for neutron irradiation in JOYO and two capsules for the out-pile tests.

Figure 5 shows a sketch of a sodium bonding irradiation capsule. Specimens were filled with liquid sodium, and were placed in a capsule component. The top-end cap was EB-welded in a vacuum. Components included

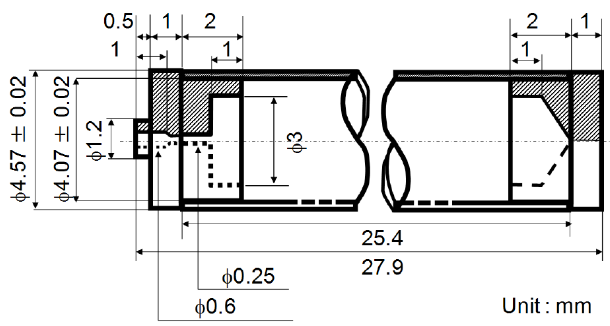

Fig. 3 Blueprint of a pressurized creep tube for a NIFS-HEAT-2 alloy.

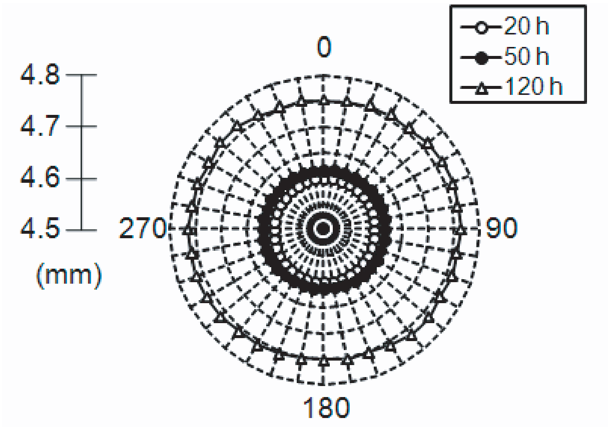

Fig. 4 Example of the creep deformation of a pressurized creep tube. The test temperature was 700°C, and the applied stress was 200 MPa.

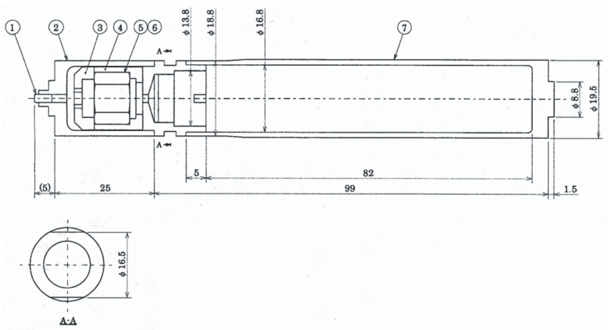

Fig. 5 Sketch of a sodium bonding irradiation capsule.

Swagelok fitting parts, which were tightened after the capsule was filled with molten sodium. Then, the outer cap and plug parts were attached by a TIG weld.

Sodium metal for filling a capsule is usually collected from a sodium storage can, and is taken to a batch bin through a riffle sampler using a unit system. As a preparatory examination, the transfer of interstitial impurity from liquid sodium metals to vanadium specimens during sodium-filling treatment was investigated. No significant changes in the concentration of oxygen and nitrogen in pure vanadium specimens were observed before or after the sodium filling treatment. Oxygen uptake from the sodium environment was up to 300-700 wppm in V-4Cr-4Ti alloys after a thermal creep test in a sodium environment.

2.4 Irradiation experiments in a sodium environment in JOYO [7]

MNTR-01 and -02 irradiations were performed for examining material irradiation in the MK-III core configuration of the JOYO reactor. The irradiation period was 2 irradiation cycles so that the effective irradiation period was 116.7 days (2802 h). Irradiation temperatures were calculated to be 458 and 598°C. The neutron doses (E > 0.1 MeV) were 6.7×10^{25} n/m^2 for the 458°C irradiation and 2.4×10^{25} n/m^2 for the 598°C irradiation. The damage levels corresponding to pure vanadium were estimated to be 1.8 dpa for 458°C and 5.0 dpa for 598°C.

After neutron irradiation, the sodium-filled capsules were disassembled, and the specimens were collected with a remnant of molten sodium. For removing these remnants, the specimens were immersed in ethanol for 2 h. After the sodium cleaning, the specimens were rinsed in an ethanol solution, and dried in a grove box. After drying, the specimens were removed from the grove box and rinsed again in air for subsequent post-irradiation experiments.

Dimensional changes of the PCTs were measured with a precision laser profilometer.

2.5 Irradiation experiments in a lithium environment in HFIR [8]

Irradiation creep experiments in a lithium environment were planned and conducted with the program used in the JUPITER-II project. HFIR-17J irradiation was performed mostly for vanadium alloy specimens in direct contact with lithium at temperatures of 450, 600, and 700°C in a europium-shielded RB position for 5 cycles for a total of 9930 MWD. Irradiation creep experiments were conducted with PCTs in the 425 and 600°C lithium-containing capsules irradiated to 3.7 dpa.

After neutron irradiation, the lithium-filled capsules were disassembled, and the specimens were rinsed with an ammonia solution to remove the molten lithium remnants completely. Dimensional changes in the PCTs were measured in ORNL with a precision laser profilometer manufactured by Z-mike.

3. Results

3.1 Thermal creep properties for NIFS-HEAT-2 alloys

Figure 6 (A) shows the time-dependence of the effective mid-wall creep strain in the temperature range of 600 to 850°C. Figure 6 (B) shows the log-log plot of Fig. 6 (A). In Fig. 6, primary creep is not observed, since the duration of primary creep is short. In previous studies employing thermal creep measurements using PCTs, no primary creep behavior was observed [8, 9]. A steady-state creep strain rate could not be obtained directly from the time-strain curve. The creep strain rate was estimated as an incline of the time-strain curve in the range from 0.1 to a few % of the creep strain.

From an Arrhenius plot of the creep strain rate obtained in Fig. 7, the activation energy for the creep of V-4Cr-4Ti was estimated for effective stress levels of approximately 100 and 150 MPa. Activation energies ranging from 197 to 227 kJ/mol were obtained, with an average value of 210 kJ/mol. The activation energies do not vary inversely with stress, as has been observed for pure vana-

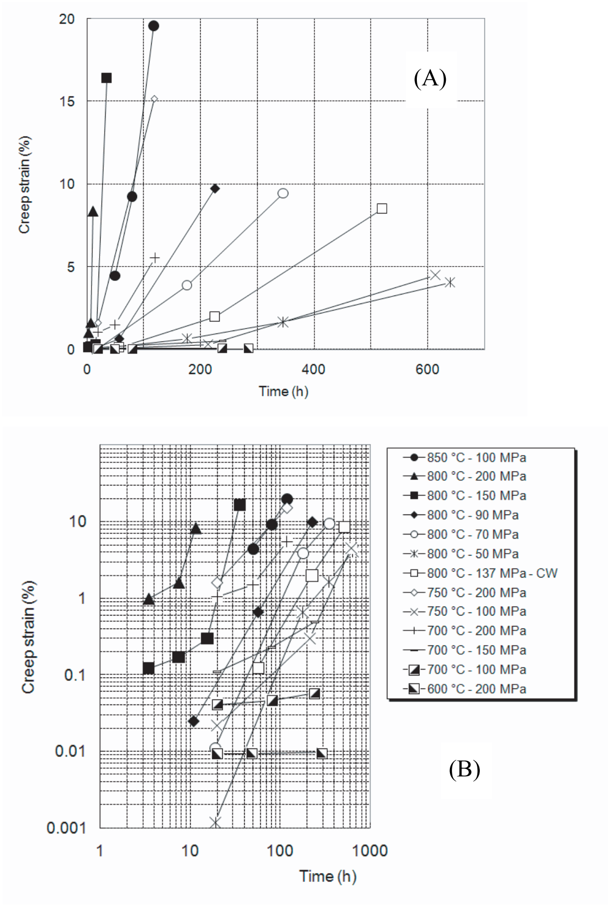

Fig. 6 Time dependence of the effective mid-wall creep strain of a highly purified V-4Cr-4Ti, with the NIFS-HEAT-2 alloy in the temperature range of 600-850°C. Fig. 6 (B) is a log-log plot of Fig. 6 (A).

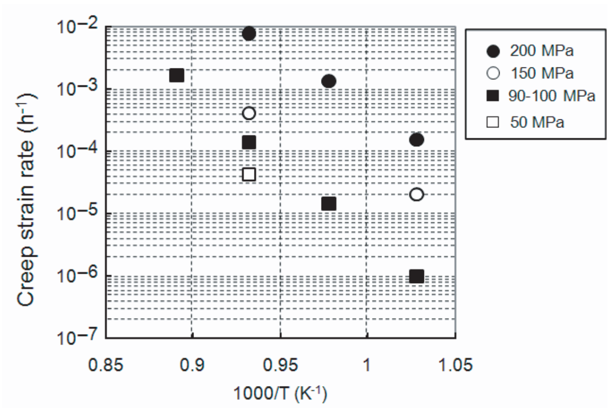

Fig. 7 Arrhenius plot of the creep strain rate of a pressurized creep tube during creep deformation in a vacuum, for NIFS-HEAT alloys. Test temperatures range from 700 to 850°C.

dium [8, 10]. These values are similar to those obtained for NIFS-HEAT in uniaxial creep tests with an activation energy of approximately 180 to 210 kJ/mol in the 750-800°C

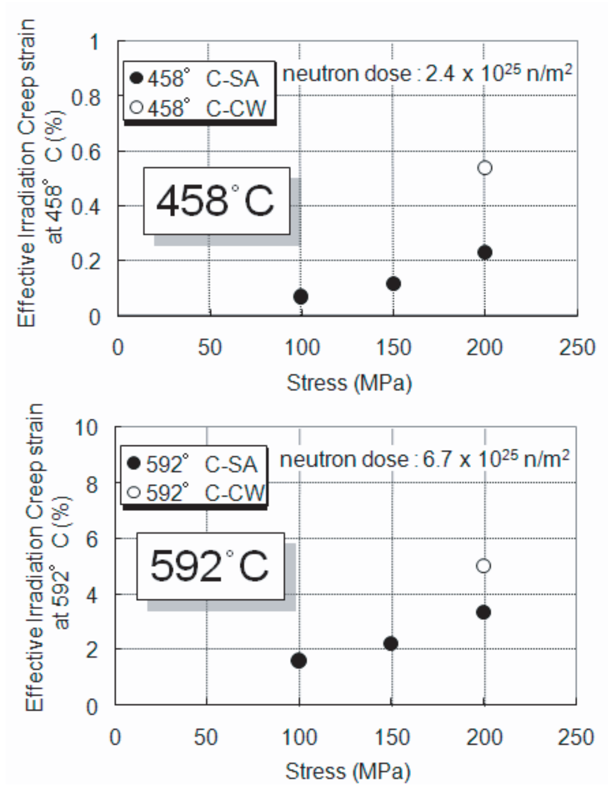

Fig. 8 Stress dependence of the effective mid-wall creep strain of a highly purified V-4Cr-4Ti, with the NIFS-HEAT-2 alloy irradiated in JOYO in a Na environment. The open circles indicate the data for cold-worked samples and the closed circles those for annealed samples.

temperature range [9]. However, these values are somewhat smaller than the activation energy for self-diffusion in pure vanadium, which is about 270 kJ/mol in the 700-800°C temperature range [8, 11].

The stress dependence of the creep strain rate is also deduced from Fig. 7. The data in Fig. 7 were fitted with the equation $d\varepsilon/dt = A\sigma^n$, where A is a constant, n is the creep stress exponent, ε is the effective creep strain rate, and σ is the effective stress. The stress exponent was determined to be 4.9 for 800°C creep data. It has been reported that the strain exponents n for pure V and V-Ti alloys [12, 13] are greater than 5 for creep test conditions similar to those used in this study, indicating that the creep mechanism is a climb-assisted glide of dislocations. The impurity uptake did not occur in creep tests with a quartz tube, because of the careful sealing treatment through chemical analysis after creep deformation tests in a vacuum.

3.2 Irradiation creep properties of NIFS-HEAT-2 alloys in a sodium environment in JOYO [7]

Figure 8 shows the plots of the effective irradiation creep strain as a function of applied stress for NIFS-HEAT alloys irradiated in JOYO in a sodium environment. It

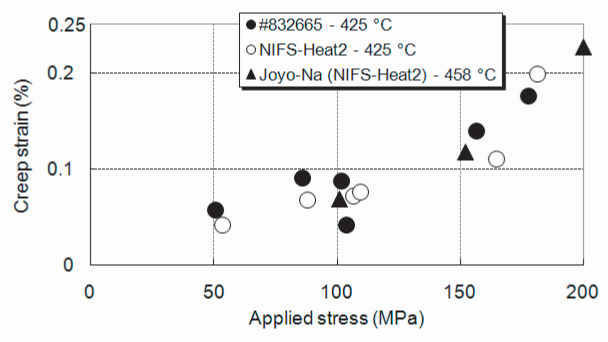

Fig. 9 Stress dependence of the effective mid-wall creep strain of a highly purified V-4Cr-4Ti, with the NIFS-HEAT-2 alloy irradiated at 425°C in HFIR-17J in a Li environment. Closed circle: #832665USA V-4Cr-4Ti alloy; open circle: NIFS-HEAT alloy; closed triangle: NIFS-heat irradiated in JOYO.

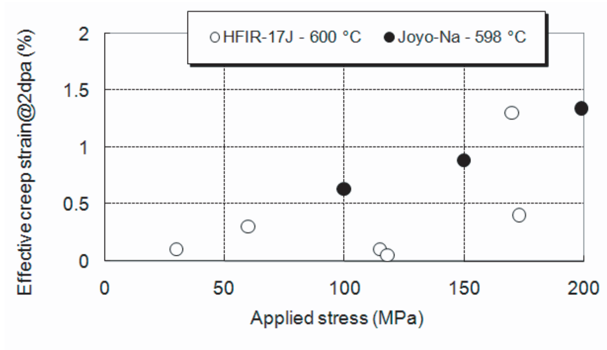

Fig. 10 Stress dependence of the effective mid-wall creep strain of a highly purified V-4Cr-4Ti, with the NIFS-HEAT-2 alloy irradiated at 600°C in HFIR-17J in a Li environment. Open circle: NIFS-HEAT alloy irradiated in HFIR; closed circle: NIFS-HEAT alloy irradiated in JOYO.

was apparent that the irradiation creep strain of the annealed V-4Cr-4Ti alloys increased proportionally with the applied stress. It is assumed that the dependence of applied stress on irradiation creep strain obey the equation $\dot{\varepsilon} \propto \sigma^n$, where n is a creep stress factor, whose value was estimated. The values of n for the annealed V-4Cr-4Ti alloys were 1.7 ± 0.3 for the 458°C irradiation and 1.1 ± 0.2 for the 598°C irradiation. Cold-worked V-4Cr-4Ti alloys exhibited a larger irradiation creep strain compared with that of the annealed V-4Cr-4Ti alloys. In a previous study of thermal creep of V-4Cr-4Ti alloys, the creep strain rate of cold-worked V-4Cr-4Ti alloys was much smaller than that of annealed V-4Cr-4Ti alloys in the temperature range of 700-800°C [8,9]. The tendency of the behavior of irradiation creep deformation in V-4Cr-4Ti alloys differed from that of thermal creep deformation during the deformation processing.

3.3 Irradiation creep properties of NIFS-HEAT-2 alloys in a lithium environment in HFIR-17J

Figure 9 shows the plots of the effective irradiation creep strain under 425°C irradiation as a function of applied stress for NIFS-HEAT alloys and #832665USA V-4Cr-4Ti alloys [8] irradiated in HFIR-17J in a lithium environment. It was apparent that the irradiation creep strain of the V-4Cr-4Ti alloys increased proportionally with the applied stress. The values of n for the NIFS-HEAT-2 alloys were approximately 1 for the 425°C irradiation. The data on creep strain for the #832662USA V-4Cr-4Ti alloys and the NIFS-HEAT alloy irradiated in JOYO at 458°C are superimposed in Fig. 9. The #832665USA V-4Cr-4Ti alloys were irradiated under the same conditions as the NIFS-HEAT alloys, and the damage level was almost the same as that for the NIFS-HEAT alloys irradiated in HFIR-17J. From Fig. 9, it can be seen that the value of the creep stress factor n at 425°C was approximately 1, below the stress level of 150 MPa. A small transition of stress dependence for irradiation creep strain can be observed at 150-160 MPa.

On the other hand, the creep strain data of the NIFS-HEAT alloy irradiated at 600°C were scattered, as shown in Fig. 10. In this figure, the plots of the effective irradiation creep strain under 600°C irradiation are shown as a function of applied stress. The data on the creep strain were converted into the creep strain rate per damage level (dpa), and plotted with the data of the NIFS-HEAT alloys irradiated in JOYO at 600°C. From the data for 600°C irradiation in Fig. 10, the higher values of irradiation creep strain rate per 2 dpa for the NIFS-HEAT alloy irradiated in HFIR-17J showed the same tendency of stress dependence of irradiation creep strain rate as for the NIFS-HEAT irradiated in JOYO. The lower value of irradiation creep strain for NIFS-HEAT irradiated in HFIR-17J may be caused by a defect in the creep tube or a malfunction of the tube during the manufacturing process, such as helium leakage at a pinhole on the tube surface of the PCTs or an unexpected uptake of interstitial impurities during the tubing process of PCT production. It was considered that the data at 30 MPa, 60 MPa, and 170 MPa were essential in determining the irradiation creep behavior of NIFS-HEAT alloys in a lithium environment.

4. Discussion

4.1 Thermal creep behavior of pressurized creep tubes

From Fig. 11, the comparison between the creep strain rate of uniaxial specimens and that of PCTs show that the uniaxial specimens deformed faster than the PCT specimens. Uniaxial tensile stress consists of only tensile stress, whereas PCT stress consists of stress resulting from both the longitudinal direction and the circumferential direction. The applied stress of PCTs was estimated by von Mises

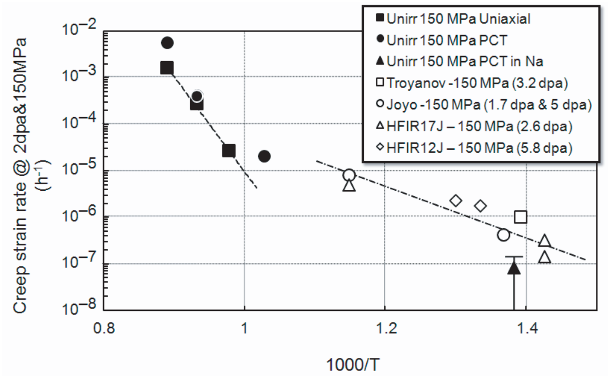

Fig. 11 Arrhenius plot of the creep strain rate for V-4Cr-4Ti alloys in a thermal creep test and an irradiation creep test. Creep strain rate values were obtained using a period of irradiation, the amplitude of the damage rate was ranged to within one order, and the stress levels of creep conditions for all data were fixed at 150 MPa.

stress, which is considered to be underestimated for comparing the absolute stress between uniaxial creep specimens and PCT specimens. The activation energy and creep stress factor for both specimen types are independent of the type of specimens, and they can be compared to investigate the essential creep behavior of the materials.

In recent studies, both uniaxial [9, 14] and biaxial [8, 15] creep tests have been performed in vacuum with differing starting concentrations of interstitial O. The apparent activation energy in the present study is 210 kJ/mol. This value is lower than the activation energy determined for the US-HEAT #832665 of V-4Cr-4Ti, 299 kJ/mol [8], and is higher than that found for V-2.8Ti, 125 kJ/mol [12, 13]. It has been reported that the strong scavenging effect of titanium and low oxygen solubility in V-3Ti corresponds to the lowest activation energy for creep in V-Ti alloys [11]. This result indicates that a reduction in matrix impurity contents may lead to lower activation energy.

4.2 Environmental effect of the irradiation creep behavior of V-4Cr-4Ti alloys

No apparent difference in the stress dependence of irradiation creep and the amplitude of irradiation creep strain rate for NIFS-HEAT alloys between JOYO irradiation and HFIR-17J irradiation was observed. The key factor in creep behavior in a liquid metal environment is the mass transfer of interstitial impurities between the bulk matrix and liquid metal. In the case of vanadium in liquid lithium, oxygen atoms move from the vanadium bulk to the liquid lithium, and nitrogen atoms move from the liquid lithium to the vanadium bulk [16]. In contrast, in the case of vanadium in liquid sodium, oxygen and nitrogen move in the opposite directions. From the comparison of irradiation creep behavior between HFIR-17J and JOYO irradiation, no characteristic difference in either irradiation creep strain rates could be seen for NIFS-HEAT alloys in this study. Therefore, the environmental effects of creep behavior due to the mass transfer of interstitial impurities is assumed to be negligible or quite small.

4.3 Irradiation creep mechanism

Figure 11 shows an Ahrrenius plot of creep strain rate. In this figure, the values of the irradiation creep strain rate were obtained using a period of irradiation, the amplitude of the damage rate was ranged within one order, and the stress levels of the creep condition for all data were fixed at 150 MPa. From Fig. 11, an activation energy for irradiation creep was estimated to be 46 kJ/mol·K. The activation energy of vacancy diffusion for the NIFS-HEAT alloy was 210 kJ/mol·K, obtained from thermal creep examination in this study.

The experimental results showed that the behavior of irradiation creep deformation was influenced by the pre-existing dislocation density, and the creep stress factor was confirmed to be in the order of 1-2. It is therefore possible that the irradiation creep mechanism in highly purified V-4Cr-4Ti alloys in the temperature range of 450-600°C is a type of stress-induced preferred absorption, (SIPA) in which the dislocation climb motion is the rate-limiting process for creep deformation assisted by the absorption of excess interstitials and vacancies in the dislocation core [17]. There is no decisive proof of the preferential absorption of point defects at dislocations during neutron irradiation, because a TEM observation of irradiation creep specimens has not yet been performed.

In the previous study, it was suggested that the irradiation creep mechanism for a NIFS-HEAT alloy is a type of irradiation-induced creep, where point defects are absorbed at the dislocation core, and that a glide dislocation movement assisted by climb motion contributes to the creep deformation [6, 7]. The irradaition creep behavior somehow involves an athermal process of creep deformation or an irradiation-induced diffusion process due to an excess concentration of point defects. It is still not clear which factor is dominant for such a rate-limiting irradiation creep deformation, but it must be related to the microstructural evolution of an irradiation-induced defect. It is therefore necessary to compare the microstructure of unloaded specimens and deformed specimens via creep tests during irradiation, and the observation of the difference in the microstructures can be used to understand the dominant factor of creep deformation during irradiation.

Consequently, the technique of sodium bond capsule irradiation in JOYO has been established. The accumulation of technical information and cumulative feedback from problems and difficulties encountered in the process are expected to be utilized to further improve the technical details of the sodium bond capsule. A set of essential physical data of irradiation creep properties was obtained in this study in order to predict the creep behavior of NIFS-HEAT alloys during neutron irradiation in a liquid metal environment, focusing on fusion reactor operations.

5. Summary

The manufacturing process of creep specimens and an irradiation technique in a liquid metal environment in-pile and creep measurements for irradiated samples were established for highly purified NIFS-HEAT alloys. Irradiation experiments with sodium-enclosed irradiation capsules in JOYO and with lithium-enclosed irradiation capsules in HFIR-17J were conducted using PCTs.

From thermal creep examination, the activation energy of creep deformation using PCTs was obtained as 210 kJ/mol·K, the creep stress factor was 4.9 for an 800°C creep test, and its mechanism was determined to be a climb-assisted glide of dislocation motion.

It was found that the creep strain rate exhibited a linear relationship, with the effective stress up to 150 MPa at 425°C and 600°C in the JOYO irradiation experiments. The creep strain rate exhibited a linear relationship, with the effective stress up to 150 MPa for HFIR-17J irradiation at 458°C. The activation energy of irradiation creep was estimated to be 46 kJ/mol·K. No significant difference in irradiation creep behavior between the liquid sodium and liquid lithium environments was observed.

Acknowledgment

This study has been conducted in collaboration with the NIFS, JAEA-Tokai and JAEA-Oarai. In particular, the authors wish to thank the members of the JOYO reactor for the irradiation operation of MNTR-01 & 02 and the members of the PIE facilities at JAEA-Oarai for the hot laboratory operation. In addition, this study has been conducted with cooperation of INITIC, JAEA in Tsuruga. This study was partly supported by NIFS Budget Code, NIFS04KFRF010. The research on the irradiation program of HFIR-17J was supported by the JUPITER-II program (Japan-USA Program of Irradiation Test for Fusion Research). One of the authors (K. Fukumoto) wishes to thank Mr. S. Sugiyama for his helpful suggestions and efforts in the manufacturing process of PCTs at IMR/Tohoku Univ.

[1] T. Muroga, J.M. Chen, V.M. Chernov *et al.*, J. Nucl. Mater. **367-370**, 386 (2007).
[2] S.J. Zinkle, H. Matsui, D.L. Smith *et al.*, J. Nucl. Mater. **258-263**, 205 (1998).
[3] K. Fukumoto, H. Matsui, M. Narui, T. Nagasaka and T. Muroga, J. Nucl. Mater. **335**, 103 (2004).
[4] T. Muroga, T. Nagasaka, A. Iiyoshi *et al.*, J. Nucl. Mater. **283-287**, 711 (2000).
[5] T. Nagasaka, T. Muroga and T. Iikubo, Fusion Sci. Tech. **44**, 465 (2003).
[6] K. Fukumoto, T. Nagasaka, T. Muroga *et al.*, J. Nucl. Mater. **367-370**, 834 (2007).
[7] K. Fukumoto, N. Narui, H. Matsui *et al.*, to be published in J. Nucl. Sci. Tech. (2008).
[8] R.J. Kurtz and M.L. Hamilton, J. Nucl. Mater. **283-287**, 628 (2000).
[9] K. Fukumoto, T. Yamamoto, S. Nakao *et al.*, J. Nucl. Mater. **307-311**, 610 (2002).
[10] K.R. Wheeler, E.R. Gilbert, F.L. Yaggee and S.A. Duran, Acta Metall. **19**, 21 (1971).
[11] D. Harrod and R.E. Gold, Int. Met. Rev. **4**, 163 (1980).
[12] H. Boehm *et al.*, J. Less-Common Met. **12**, 280 (1967).
[13] H. Boehm *et al.*, Z. Metallkdet. **59**, 715 (1968).
[14] K. Natesan, W.K. Soppet and A. Purohit, J. Nucl. Mater. **307-311**, 585 (2002).
[15] R.J. Kurtz, K. Abe, V.M. Chernov *et al.*, J. Nucl. Mater. **329-333**, 47 (2004).
[16] D.L. Smith and K. Natesan, Nucl. Technol. **32**, 392 (1974).
[17] L.K. Manser and T.C. Reiley, J. Nucl. Mater. **90**, 60 (1980).